

# Transient Model of an RSW System with CO<sub>2</sub> Refrigeration – A Study of Overall Performance

Eivind Brodal\*, Steve Jackson and Oddmar Eiksund

UiT-The Arctic University of Norway, NO-9037 Tromsø, Norway

## Abstract

Refrigerated seawater (RSW) cooling using CO<sub>2</sub> based refrigeration is a relatively new technology that shows promising performance in cold climates. For being a refrigerant CO<sub>2</sub> has a low global warming potential (GWP) and is therefore recognized as an environmentally friendly alternative if the unit is competitive on energy efficiency. However, RSW systems with CO<sub>2</sub> have a significant reduction in energy efficiency if operated in warm seawater due to its low critical temperature. This study investigates the impact ambient temperature and precooling processes have on performance. The results show that for a fixed process design, lower ambient temperature in the Barents Sea results in an average COP of 5.0 compared with 3.0 to 3.5 in the Mediterranean Sea, or alternatively, that a ship can operate with RSW tanks that are approximately three times bigger if ambient seawater temperature is 10° C compared to 20° C. The study also finds that for a fixed ambient temperature case, the RSW tank can be 3.6 to 1.8 times larger if one third of the tank volume is precooled.

## Keywords

RSW; COP; CO<sub>2</sub>; Seawater temperature

\* Corresponding author. Tel.: +47 77660364. E-mail: [eivind.brodal@uit.no](mailto:eivind.brodal@uit.no)

## Nomenclature

Symbols		Subscripts & Superscripts	
COP	Coefficient of performance [-]	0	Time when the fish are added
$c$	Specific heat capacity [J/(kgK)]	av	Average
$h$	Specific enthalpy [kJ/kg]	comp	Compressor property
$\dot{m}$	Mass flow rate [kg/s]	crit	Critical property
$m$	Mass [kg]	E	Evaporator property
$P$	Duty [kW]	end	End time (i.e. tank temperature 0 °C condition)
$p$	Pressure [bar]	is	Isentropic
SST	Sea surface temperatures [°C]	max	Max property
$T$	Temperature [°C]	S	Displacement (i.e. displacement flow property)
$t$	Time [s]	start	Cooling start time condition
$\dot{V}$	Volume flow [m <sup>3</sup> /s]	std	Standard
$V$	Volume [m <sup>3</sup> ]	super	Superheat condition
$\eta$	Efficiency [-]	SW	Seawater property
$\lambda$	Volumetric efficiency [-]	tank	Seawater tank property
$\rho$	Density [kg/m <sup>3</sup> ]		

# 1 Introduction

Chilling fish in refrigerated seawater (RSW) is an important conservation method in the fish industry, having cooling capacities up to 1500 kW. Big factory ships have more than 1000 m<sup>3</sup> of refrigerated tanks. In 2000, 90% of Norwegian ships longer than 21 meters were equipped with mechanical refrigeration (Hansen, 2000). RSW technology is also used for conservation in land based food industry (Widell and Eikevik, 2010). Systems conserving seafood have to follow food industry regulation like the EU Council Directive (92/48/EEC), which states “The operation of the tank or container system must secure a chilling rate which ensures the mix of fish and seawater reaches 3° C at the most six hours after loading and 0° C at the most after sixteen hours.”

Environmental regulations are driving technology development. In 2006 around 70 to 80 % of merchant fishing and naval vessels used HCFC-22 as a refrigerant, while the rest were HFCs and ammonia (NH<sub>3</sub>) based (United Nations Environment Programme (UNEP), 2006). HCFC-22 will according to the Montreal protocol be eliminated by 2030. In the EU and Norway this regulation was already introduced in 2010 (Skiple, 2008). International treaties and national laws have made natural refrigerants, like CO<sub>2</sub> and NH<sub>3</sub>, popular to use in a large variety of applications since they have almost negligible impacts on the environment (Hansen, 2000; Kim et al., 2004; Pedersen, 2014).

The fishing industry is also adapting to the new environmentally friendly technologies (Ruiz, 2012), and the first commercial CO<sub>2</sub> based RSW boat system in the world was installed in the vessel Båragutt MS in 2010 by Kuldeteknik AS, based in Northern Norway (Pedersen, 2014). CO<sub>2</sub> compressors require relatively low swept volumes due to high evaporating pressure, and have advantages over e.g. NH<sub>3</sub>, which is toxic, moderately flammable and reacts with copper and copper alloys. Hansen states that RSW units with CO<sub>2</sub> are more efficient than HCFC-22 in cold climates, and claims that this occurs for condensing temperatures below 21° C (Hansen, 2000). Compared to other technologies, CO<sub>2</sub> based RSW units have a significant reduction in efficiency and cooling capacity if operated in warm seawater, which can be explained by the low critical temperature  $T_{\text{crit}} = 31.0^{\circ}\text{C}$  (critical pressure is  $p_{\text{crit}} = 73.8\text{ bar}$ ) of CO<sub>2</sub> (Kim et al., 2004).

Currently, little research work is identified investigating variation in overall performance of RSW units with ambient seawater temperature, or relating performance to geographical location. Ambient temperature is crucial when studying RSW performance and plays important roles throughout the process (Kolbe, 1990), since seawater is used as a cooling medium in the gas cooler and seawater and fish are added to the RSW tank, and then cooled down to storage temperature. Much research on refrigeration cycle performance has been published and some in connection with RSW performance. Wang and Wang, 2005, have published a study of recent developments in fishing refrigeration technology. Temperature variation during RSW tank processes have been documented experimentally with temperature loggers (Tveit et al., 2015). Others have used a transient model to investigate temperature variation during a cooling process for 17° C seawater (Thorsteinsson et al., 2003). Designs of CO<sub>2</sub> based RSW systems, and experimental data obtained from a test rig are discussed in (Gilberg, 2011). Pigani et al. published a large study comparing current marine refrigeration units and systems with low GWP refrigerants (Pigani et al., 2016), but only studied cases with high seawater temperatures, above 18° C, which is equivalent to a 31.5° C condensing temperature since their model assumed a 13.5 K temperature difference.

Much of the literature describing refrigeration performance and variation in ambient temperature is based on an assumption of constant temperature difference between the refrigerant exiting the

condenser and ambient temperature e.g. seawater, independent of the refrigerant and process conditions. Such an approach has also been applied in comparative studies of refrigerants, including CO<sub>2</sub>, e.g. in (Hansen, 2000; Pigani et al., 2016). However, comparing systems with the same evaporator and condensing temperatures may potentially underestimate the heat exchanger performance in the CO<sub>2</sub> systems because CO<sub>2</sub> operates at particularly high densities and pressures. An original aspect of the present study is the use of detailed exchangers models instead of fixed temperature approaches. This is important because the RSW refrigeration unit is modeled for all ocean temperatures, i.e. over a large water temperature range, from freezing to 35° C, on both the gas cooler and evaporator side.

CO<sub>2</sub> based RSW systems are relatively new to the industry, and this article describes how the temperature of ambient seawater effects cooling capacity and coefficient of performance (COP). This information is linked to geographical locations, and used to investigate the conditions under which CO<sub>2</sub> based RSW systems could have a performance advantage. Performance data is obtained using an original approach that combines the specific operating conditions found in RSW systems on board fishing vessels with a system model that includes detailed heat exchanger models and EN12900 based compressor performance data. This process model is developed using the process modeling software HYSYS.

## 2 RSW Design, Specifications and Method

There are many different possible designs for an RSW system on board a ship (Gilberg, 2011). In this article, a CO<sub>2</sub> based refrigeration cycle with relatively few components, as shown in Figure 1, is studied. This is a system with an in-line medium-pressure receiver (Kim et al., 2004), and can operate both transcritical and subcritical. The quality and size of the individual components integrated in the system effects the performance.

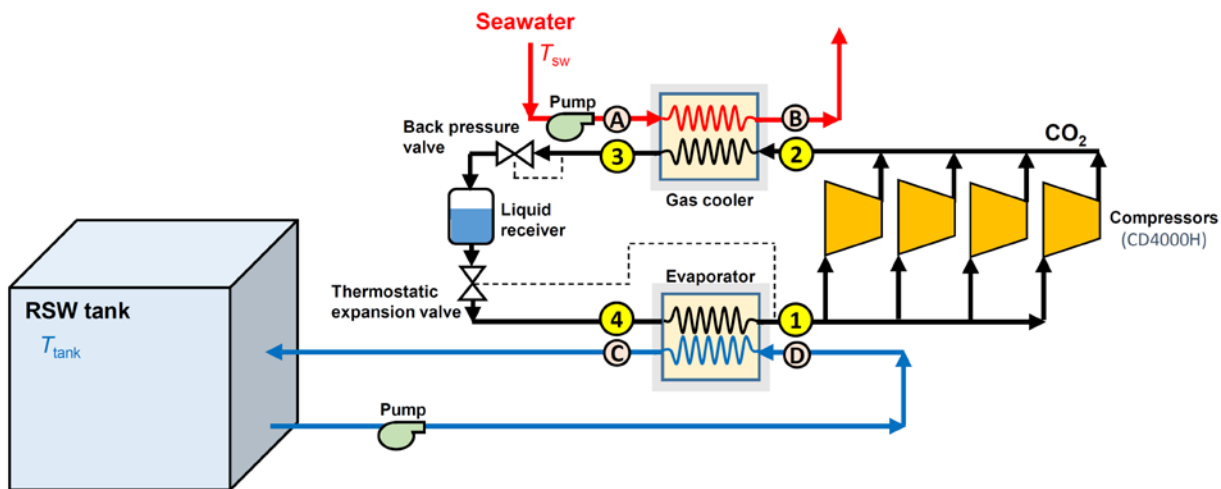


Figure 1. Flow diagram of the RSW tank and the refrigeration unit using CO<sub>2</sub> refrigerant and four CD4000H compressors.

A model of the RSW unit was created to investigate performance at different geographical locations for two RSW tank filling approaches. This model was developed through five main modulation stages:

1. Implement experimental based compressor performance data provided by manufacturer.
2. Size the heat exchangers (evaporator and gas cooler).
3. Create a static model of the refrigeration cycle (both subcritical and transcritical).
4. Create a transient model of the RSW tank filling based on data from the static model.
5. Combine the modeled performance data with global surface seawater temperature (SST) data.

HYSYS is used for process modelling purposes in this study because it allows process performance to be combined with detailed compressor and exchanger performance models. HYSYS is a leading process simulation software package that is provided by Aspentech.

## 2.1 Process Specifications

The system is sized to produce around 300 kW cooling capacity when  $T_D \approx T_{\text{tank}} = 0^\circ \text{C}$  and  $T_A \approx T_{\text{sw}} = 20^\circ \text{C}$ , which is a realistic sized RSW unit (Kuldeteknisk AS, 2017). Component description and refrigeration cycle specification are given below:

- The thermostatic expansion valve regulates a 4 K superheat ( $T_{\text{super}}$ ) to prevent liquid from entering the compressors.
- Four CD4000H compressors working in parallel to achieve the desired cooling capacity.
- Shell and tube evaporator with titanium tubes. CO<sub>2</sub> on the shell side. Titanium is used because it offers benefits in seawater applications such as: low rates of corrosion and erosion, high allowable water velocities and low fouling rates.
- Titanium shell and tube gas cooler with tube inserts to increase heat exchanger performance. CO<sub>2</sub> on the tube side. Operates as a condenser if  $p_3$  is less than critical pressure.
- Liquid receiver providing CO<sub>2</sub> at bubble point to the thermostatic expansion valve.
- The backpressure valve regulates the high pressure, and is set to  $p_2$  that generates maximum COP. If the process is subcritical, it is open (zero pressure drop).
- Pumps generate constant volume flow ( $\dot{m}_A = 16.4 \text{ kg/s}$  and  $\dot{m}_D = 58.3 \text{ kg/s}$ ).

The thermal properties of seawater vary (Sharqawy et al., 2010), in this work, seawater is assumed to have 35 g/kg salinity. Property values from the HYSYS property library are used for CO<sub>2</sub>, titanium and seawater in the HYSYS model.

The main aim is to investigate relative performance of a fixed system design with varying seawater temperatures. Some simplifications were made in order to keep the system as simple as possible in the modulation work.

### Simplifications in the Modelling Work

Perfect insulated RSW tanks with uniform water temperature is assumed, and both seawater and fish are modeled with specific heat capacity  $c_{\text{sw}} = 4005 \text{ J/(kgK)}$  and mass density  $\rho_{\text{sw}} = 1026 \text{ kg/m}^3$  in the post processing work of the steady state performance data calculated in HYSYS. A uniform temperature in the RSW tank is assumed, since temperature variations typically are small (Tveit et al., 2015). It is also assumed that the heat exchangers are clean (zero fouling factor). The performance depends on the history of the RSW unit, due to fouling in the heat exchangers. However, fouled tubes can return to almost “new” if they are cleaned mechanically or chemically (Lindeburg, 2013).

Only full load cases are studied. That is, the pumps and the four compressors are always working at design speed. Turning off or reducing compressor speed is necessary when the RSW tank water is cooled down to the desired temperature to maintain a constant low temperature at reduced cooling duty. However, the pump filling the RSW tank is allowed to be regulated in the post processing work, since none of the specifications described above prevent the CO<sub>2</sub> pressure at the compressor inlet ( $p_1$ ) to be higher than the compressor design limit. Another approach, to operate within the compressor design

limit, is to reduce the water flow through the evaporator by regulating the water pump, but this falls outside of the scope of the present study.

## 2.2 Refrigeration Cycle and Component Performance

The efficiency of a refrigeration cycle is typically described by the coefficient of performance:

$$\text{COP} = \frac{P_E}{P_{\text{comp}}} = \frac{h_1 - h_4}{h_2 - h_1}, \quad (1)$$

where  $h$  is enthalpy,  $P_E$  is the cooling capacity,  $P_{\text{comp}}$  is the energy consumptions of the compressor. The same numbering convention as in Figure 1 is used. Energy consumption of the whole RSW unit will also include other energy consumption such as the water pumps. Compressor performance is often described by isentropic ( $\eta$ ) and volumetric ( $\lambda$ ) efficiencies:

$$\eta = \frac{P_{\text{comp, is}}}{P_{\text{comp}}} = \frac{h_{2is} - h_1}{h_2 - h_1} \quad (2)$$

$$\lambda = \frac{\dot{V}_1}{\dot{V}_s} = \frac{\dot{m}_1}{\rho_1 \dot{V}_s}, \quad (3)$$

where  $\dot{m}_1$  is the CO<sub>2</sub> mass flow,  $\dot{V}_s$  is the physical displacement volume per second in the compressor and  $P_{\text{comp, is}}$  is an isentropic compression process.

The refrigeration process depends on seawater temperature  $T_{\text{sw}}$  and the RSW tank temperature  $T_{\text{tank}}$ , and temperature differences in the heat exchangers are related to thermodynamic loss. In this work, accurate models of the exchangers are applied through design dependent inputs. The differences ( $T_3 - T_{\text{sw}}$ ) and ( $T_{\text{tank}} - T_4$ ) are used as condition based measurements of heat exchanger performance for the gas cooler and the evaporator, respectively.

## 2.3 Component Specification and Performance

The specifications and performance of the key components (compressors, gas cooler, evaporator and back pressure valve) are integrated in the modelling work, as described below.

### 2.3.1 Compressors

The CD4000H model from DORIN is chosen in this study. This is a 199 kg semi-hermetic CO<sub>2</sub> piston compressor which can operate transcritically (above critical pressure  $p_{\text{crit}}$ ). This model has 4 cylinders, 45 mm bore and 48 mm stroke and operates at 50 Hz, which gives a displacement volume flow of  $\dot{V}_s = 26.57 \text{ m}^3/\text{h}$ . However, the CD4000H model can only operate at evaporating temperatures ( $T_E = T_1 - T_{\text{super}}$ ) between -30° C and 15° C (Wolf, 2015). DORIN CO<sub>2</sub> piston compressors were used in the vessel Båragutt MS (Gilberg, 2011).

#### Factory Performance Data

EN12900 is a standard that defines “rating conditions, tolerances and presentation of manufacturer's performance data” for refrigeration compressors, and is based on 10 K superheat for CO<sub>2</sub> compressors. Following the EN12900 standard, DORIN provides formulas describing the compressor power consumption ( $P_{\text{comp, std}}$ ) and mass flow ( $\dot{m}_{\text{std}}$ ) for the compressor (Wolf, 2015):

$$P_{\text{comp, std}}(T_E, p_2) = c_1 + c_2 T_E + c_3 p_2 + c_4 T_E^2 + c_5 T_E p_2 + c_6 p_2^2 \quad (4)$$

$$\dot{m}_{\text{std}}(T_E, p_2) = c_1 + c_2 T_E + c_3 p_2 + c_4 T_E^2 + c_5 T_E p_2 + c_6 p_2^2 + c_7 T_E^3 + c_8 T_E^2 p_2 + c_9 T_E p_2^2 + c_{10} p_2^3, \quad (5)$$

here the coefficients are obtained from the “DORIN Software” (Wolf, 2015), and are given in Table 1. For non-standard superheating conditions ( $T_{\text{super}} \neq 10$  K), DORIN informed via email that they use the performance model:

$$P_{\text{comp}}(T_E, p_2, T_{\text{super}}) = P_{\text{comp, std}}(T_E, p_2) \quad (6)$$

$$\dot{m}_1(T_E, p_2, T_{\text{super}}) = \dot{m}_{1, \text{std}}(T_E, p_2) \cdot \left( 1 + \left( a_k \cdot \frac{p_2}{p_1} + c_k \right) \cdot \left( \frac{\rho_1}{\rho_{1, \text{std}}} - 1 \right) \right), \quad (7)$$

where  $a_k = -0.02$  and  $c_k = 1.04$  are experimentally determined correction factors for CO<sub>2</sub> compressors, and  $\rho_1$  is the suction mass density. Equations (4) – (7) are only valid in the compressors operating range ( $-30^\circ \text{C} \leq T_E \leq 15^\circ \text{C}$ ). Figure 2 illustrates operating range, as well as isentropic and volumetric efficiency.

Table 1. Coefficients used in Eqs.(4) – (5) for the 50Hz CD4000H compressor.

	C1	C2	C3	C4	C5	C6	C7	C8	C9	C10
$\dot{m}_{1, \text{std}}$ [kg/s]	6,99E-1	1,87E-2	-2,86E-3	1,70E-4	-1,42E-5	9,45E-6	-	-	-	-
$P_{\text{comp, std}}$ [W]	-3,14E4	-1,11E3	1,29E3	-1,08E1	1,62E1	-8,85E0	-1,20E-2	3,00E-2	-4,52E-2	2,61E-2

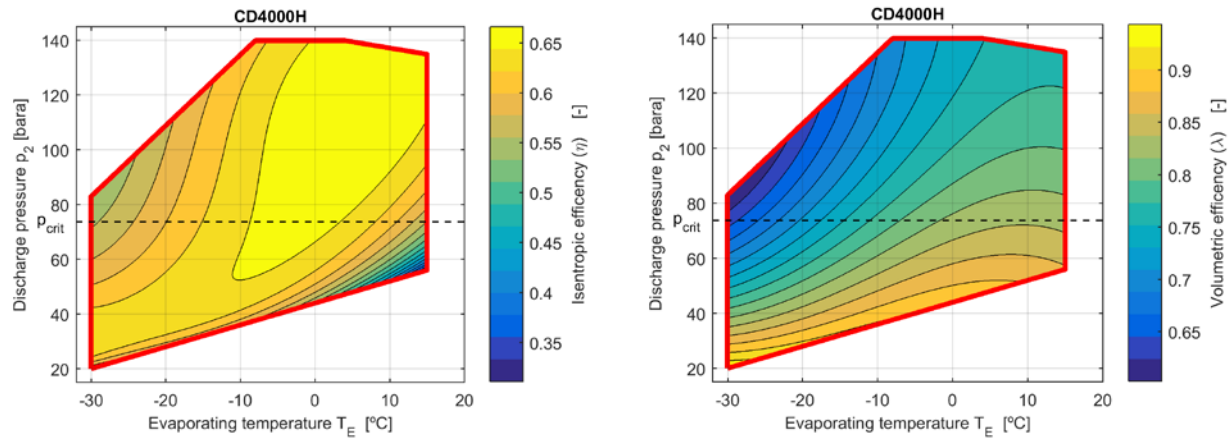


Figure 2. Isentropic and volumetric efficiency of the CD4000H compressor (with 4K superheat) calculated using CoolProp, compressor performance data from Eqs.(6) – (7) and the operating range described in Wolf, 2015.

### 2.3.2 Evaporator and Gas Cooler Specifications and Performance

In this study, single-pass straight tubes are modelled giving true counter current flow, good accessibility for inspection and easy cleaning. The design of the heat exchangers was created by inserting process specifications into HYSYS (for 20° C seawater and 0° C tank water), and then using the “Auto sizing” routine in the “Rigorous shell & tube” heat exchanger model to find a practical and efficient design, as shown in Figure 3 and Table 2. The “Rigorous shell & tube” heat exchanger model is based on a HTFS sizing algorithm which includes pressure drop in heads, nozzles and lines, and has a material property library which includes Titanium. Default tube wall roughness of 0.003 mm was used. It is normal practice to use tube inserts in the gas cooler to increase turbulence and the heat transfer coefficient (Gilberg, 2011). The pressure drop and the optimal tube insert dimensions depend on both the RSW tank temperature and the seawater temperature. Tube inserts with dimensions that create between 0.60 and 1.5 bar pressure drops in the gas cooler for subcritical processes were used, and between 0.24 and 1.1 bar in the transcritical processes.

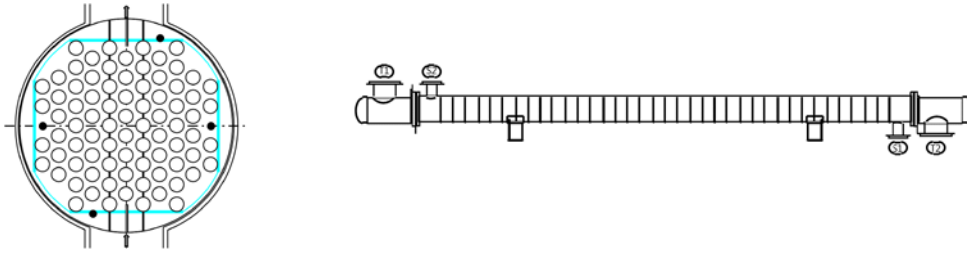


Figure 3. The evaporator's tube and shell layout. (Figures are created by the "Rigorous shell & tube" model in HYSYS.)

Table 2. Heat exchanger specifications. The layout of the evaporator is shown in Figure 3.

	Shell and tube evaporator	Shell and tube gas cooler
Material	Titanium	Titanium
Tube side fluid	Seawater (from RSW tank)	CO <sub>2</sub>
Shell side fluid	CO <sub>2</sub>	Seawater (from ocean)
Tube outer diameter $d_o$	19.05 mm	19.05 mm
Tube inner diameter $d_i$	16.57 mm	16.57 mm
Tube pitch	23.81 mm	23.81 mm
Tube length	5.00 m	4.00 m
Number of tubes	80	60
Tube inserts (Twisted tape)	-	Thickness 4.00 mm 12 mm twist pitch per 360°
Baffle number (cut%)	37 (42%)	20 (40%)
Shell inner diameter $d_i$	264.67 mm	300.00 mm
Tube passes	1	1

## Modelled Performance

Figure 4 shows temperature profiles generating the heat transfers in the evaporator and gas cooler described in Table 2, using real compressor performance data and the "Rigorous shell & tube" model in HYSYS.

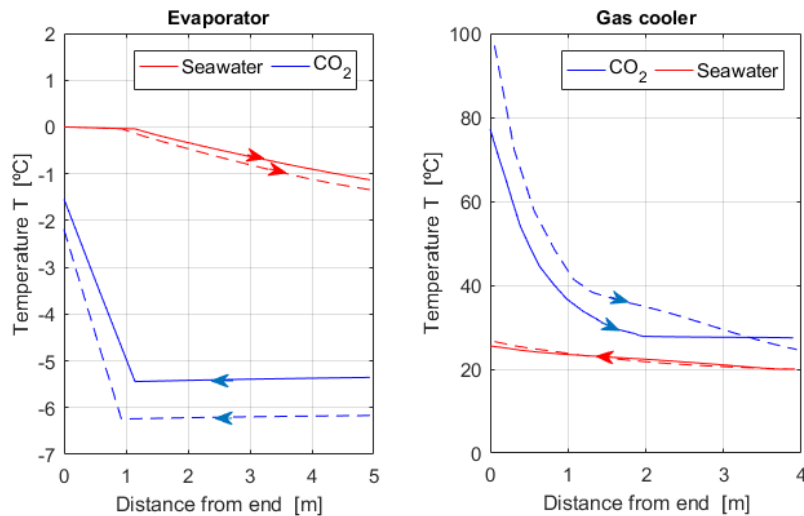


Figure 4. Temperature profiles for subcritical (solid lines) and transcritical (dashed lines) processes in the evaporator and gas cooler when  $T_{tank} = 0.0^\circ\text{C}$  and  $T_{sw} = 20.0^\circ\text{C}$ .



## 2.4 Steady State RSW Model

HYSYS is used to model the steady state performance of the refrigeration cycle when operating with different seawater and tank temperatures  $P_E(T_{sw}, T_{tank})$  and  $COP(T_{sw}, T_{tank})$ . The different points in the refrigeration cycle are computed in the model as follows:

- **Point 1:**  $T_1$  and  $p_1$  are calculated by the “Rigorous shell & tube” heat exchanger model based on evaporator design information, mass flows and the thermodynamically properties from “Point 4” and “Point D”.
- **Point 2:**  $T_2$  is calculated from  $p_2$  and “Point 1” using the compressor model described in Eqs. (4) to (7).
- **Point 3:**  $T_3$  and  $p_3$  are calculated by the “Rigorous shell & tube” heat exchanger model, which includes gas cooler design information, mass flows and the thermodynamically properties of “Point 2” and “Point A”.
- **Point 4:**  $T_3$  is calculated from  $p_4$  and “Point 3” through a constant enthalpy flash process.

The presence of the liquid receiver and the regulated superheating of the thermostatic expansion valve give two additional constraints for the steady state process. The compressor model described in Eqs. (4) to (7) is used to compute  $\dot{m}_1$  and  $P_{comp}$  from  $T_1$  and  $p_2$ . However,  $T_1$  and  $p_2$  cannot be calculated directly by HYSYS because both of the heat exchanger models require an initial value for  $\dot{m}_1$  at “Point 2” and “Point 4” to calculate outlet conditions. An iteration is, therefore, made until the guessed and calculated values for  $\dot{m}_1$  match.

In order to solve the subcritical problem, the steady state pressures  $p_4$  and  $p_2$  are also computed through iterations from an initial guess until also the bubble point and superheat conditions are satisfied, as explained in Table 3. In the transcritical processes, the operating pressure  $p_2$  is optimized with respect to COP using the HYSYS “Original” optimizer data model. Otherwise, the model is identical. The most efficient operating condition overall is found by comparing calculated COP values for both the subcritical and the optimized transcritical process.

Table 3. Model specifications of  $p_4$  and  $p_2$ .

Subcritical	Transcritical
$p_2$ is adjusted through iterations in HYSYS so that “Point 3” is at bubble point.	$p_2$ is optimized for maximum COP at the current operating conditions.
$p_4$ is adjusted through iterations in HYSYS so that “Point 1” is superheated with 4 K.	Same as subcritical.

Peng Robinson properties package is used to calculate the energy balance, and the “Standard method” is used to solve the “Rigorous shell & tube” heat exchanger model.

## 2.5 Modeling Transient Chilling Processes

The RSW tank temperature  $T_{tank}(t)$  varies over time during the cooling process, and depends on seawater temperature  $T_{sw}$ , refrigeration duty  $P_E(T_{sw}, T_{tank}(t))$  and the RSW tank size  $V_{tank}$ . The EU Council Directive (92/48/EEC), requirements of reaching 3° C in six hours and 0° C in 16 hours creates an upper limit on the RSW tank size (for given seawater temperature). In this work, RSW units with maximum RSW tank size  $V_{tank}^{max}$  are used as base cases when comparing performance.

To explore the limits of system performance, two RSW filling cases are studied, where it is assumed that it takes one hour to add  $V_{tank}/3$  of seawater or fish to the RSW tank:

- Case A: an empty RSW tank is filled. The refrigeration unit is turned on when the RSW tank is full.
- Case B:  $V_{tank}/3$  of seawater is precooled to 0° C. Fish and more seawater at  $T_{sw}$  is added during a two hour period until the tank is full.



In “Case B”, the precooling starts with a 1/3 full RSW tank in cold waters, but, in order to be able to operate within the compressor limitation ( $T_E \leq 15^\circ \text{C}$ ) in warm waters ( $T_{sw} > 20^\circ \text{C}$ ), the tank temperature is kept at  $T_{\text{tank}} = 20^\circ \text{C}$  in the beginning of the precooling process by reducing the RSW tank filling rate.

Refrigeration starts at time  $t_{\text{start}}$ , the first fish are added at  $t_0 = 0 \text{ s}$  and then cooled down to  $0^\circ \text{C}$ . The mass of the water and fish in the tank  $m_{\text{RSW}}(t, V_{\text{tank}})$  depends on both time and the RSW tank size. The temperature for a given RSW tank size is given as an initial value problem:

$$T_{\text{tank}}(t) = T_{\text{sw}} - \frac{\int_{t_{\text{start}}}^t P_E(T_{\text{sw}}, T_{\text{tank}}(t')) dt'}{m_{\text{RSW}}(t, V_{\text{tank}}) \cdot c_{\text{sw}}} = T_{\text{sw}} - \frac{1}{c_{\text{sw}}} \int_{t_{\text{start}}}^t \frac{P_E(T_{\text{sw}}, T_{\text{tank}}(t'))}{\dot{m}_{\text{RSW}}(t', V_{\text{tank}})} dt', \quad (8)$$

which is solved numerically to find the time the temperature reaches  $3^\circ \text{C}$  ( $t_{3^\circ \text{C}}$ ) and  $0^\circ \text{C}$  ( $t_{\text{end}}$ ). Viewing  $t_{3^\circ \text{C}}$  and  $t_{\text{end}}$  as functions of tank volume, the maximum RSW tank sizes ( $V_{\text{tank}, 3^\circ \text{C}}^{\text{max}}$  and  $V_{\text{tank}, 0^\circ \text{C}}^{\text{max}}$ ) for each of the required conditions is found numerically by inverting these functions at  $t_{3^\circ \text{C}} = 6 \text{ h}$  and  $t_{\text{end}} = 16 \text{ h}$ . The RSW unit must fulfill both conditions, i.e. the maximum RSW tank size  $V_{\text{tank}}^{\text{max}} = \min(V_{\text{tank}, 3^\circ \text{C}}^{\text{max}}, V_{\text{tank}, 0^\circ \text{C}}^{\text{max}})$ . The average cooling capacity and COP are given by the integrals:

$$P_{E, \text{av}}(T_{\text{sw}}, V_{\text{tank}}^{\text{max}}) = \frac{\int_{t_{\text{start}}}^{t_{\text{end}}} P_E(T_{\text{sw}}, T_{\text{tank}}(t')) dt'}{t_{\text{end}} - t_{\text{start}}} \quad (9)$$

$$\text{COP}_{\text{av}}(T_{\text{sw}}, V_{\text{tank}}^{\text{max}}) = \frac{\int_{t_{\text{start}}}^{t_{\text{end}}} P_E(T_{\text{sw}}, T_{\text{tank}}(t')) dt'}{\int_{t_{\text{start}}}^{t_{\text{end}}} P_{\text{comp}}(T_{\text{sw}}, T_{\text{tank}}(t')) dt'} = \frac{\int_{t_{\text{start}}}^{t_{\text{end}}} P_E(T_{\text{sw}}, T_{\text{tank}}(t')) dt'}{\int_{t_{\text{start}}}^{t_{\text{end}}} \frac{P_E(T_{\text{sw}}, T_{\text{tank}}(t'))}{\text{COP}(T_{\text{sw}}, T_{\text{tank}}(t'))} dt'} \quad (10)$$

which are computed numerically using  $P_E(T_{\text{sw}}, T_{\text{tank}})$  and  $\text{COP}(T_{\text{sw}}, T_{\text{tank}})$  from the steady state model.

## 2.6 Sea Surface Temperature Data

The Japan Meteorological Agency (JMA) provides monthly global sea surface temperature (SST) data with a resolution of  $1^\circ$  latitude and  $1^\circ$  longitude (Japan Meteorological Agency, 2006). Maximum ( $\text{SST}_{\text{max}}$ ) and average ( $\text{SST}_{\text{av}}$ ) are computed from the monthly SST data (for 2016) downloaded from JMA website Japan Meteorological Agency, and have formed the basis for modelling the geographic performance for “Case A” and “Case B”. Average COP values are interpolated from the different location’s average  $\text{SST}_{\text{av}}$ . The maximum RSW tank volume, which is a limiting factor for the RSW unit is computed at different geographical locations by combining modeled performance data and the location’s maximum  $\text{SST}_{\text{max}}$ . The RSW units performances are illustrated in detailed maps of the world created using MATLAB built in map function “contourfm”.

## 3 Results

The results of this study are shown below in three parts. The first part presents the steady state performance of the RSW system for different tank and ambient seawater temperatures; the second part presents average performance parameters calculated from the transient model of the cooldown process; the last part presents the overall performance at different geographical locations.

### 3.1 Steady State RSW Performance Data (HYSYS Model)

The performance of the refrigeration process for different conditions is computed in the HYSYS model. Five examples of modelled values are shown in Table 3, using the notation illustrated in Figure 1. The cooling duty  $P_E(T_{\text{sw}}, T_{\text{tank}})$  and  $\text{COP}(T_{\text{sw}}, T_{\text{tank}})$  for the relevant temperature ranges are given in Figure 5. Only transcritical processes are possible in warmer seawaters above  $22^\circ \text{C}$ . At lower temperatures, both

transcritical and subcritical processes are shown. In Figure 5, however, the RSW unit is regulated to operate with the process that has the best COP.

In all cases, the seawater pumps run with constant flow:  $\dot{m}_A = 16.4 \text{ kg/s}$  and  $\dot{m}_D = 58.3 \text{ kg/s}$ , which generates constant pressure drops:  $p_A - p_B = 0.45 \text{ bar}$  over the evaporator and  $p_C - p_D = 0.49 \text{ bar}$  pressure drop over the gas cooler.

Table 3. Modeled process data for different  $T_{sw}$  and  $T_{tank}$ .

$T_{sw}$ [°C]	20.0	20.0	35.0	10.0	35.0
$T_{tank}$ [°C]	0.0	0.0	0.0	10.0	20.0
Running mode	Subcritical	Transcritical	Transcritical	Subcritical	Transcritical
$T_1$ [°C]	-1.5	-2.2	-0.3	7.1	19.2
$T_2$ [°C]	77.1	97.6	94.5	54.4	67.0
$T_3$ [°C]	27.5	24.7	37.5	22.3	38.9
$T_4$ [°C]	-5.3	-6.2	-4.2	3.1	15.4
$p_1$ [bar]	29.6	29.0	30.6	37.4	51.0
$p_2$ [bar]	68.9	83.1	83.7	62.0	85.5
$p_2 - p_3$ [bar]	0.65	0.31	0.35	1.34	0.82
$p_4 - p_1$ [bar]	0.11	0.09	0.13	0.16	0.24
$\dot{m}_1$ [kg/s]	1.91	1.78	1.91	2.60	3.62
$T_B$ [°C]	25.5	26.6	39.0	17.7	39.8
$T_C$ [°C]	-1.1	-1.3	-0.6	8.2	19.2
$P_E$ [kW]	264	314	144	426	206
COP [-]	2.67	2.64	1.21	5.38	1.87

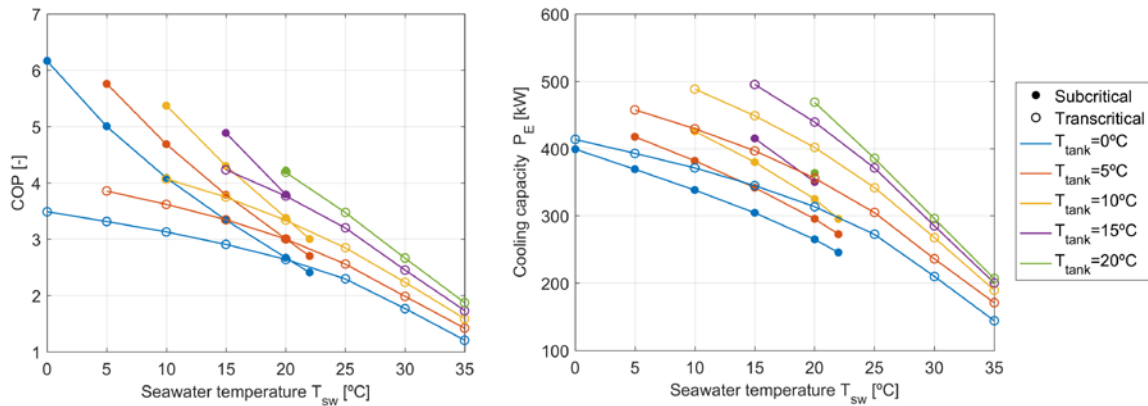


Figure 5. COP and cooling capacity for different tank and sea temperatures.

Figure 6 illustrates the temperature difference ( $T_3 - T_{sw}$ ) for the gas cooler and ( $T_{tank} - T_4$ ) for the evaporator at different conditions.

The condensing temperature is shown in Figure 7, where  $T_3 = 21^\circ \text{C}$  is indicated since  $\text{CO}_2$  have been claimed to be more efficient than HCFC-22 below this temperature (Hansen, 2000).

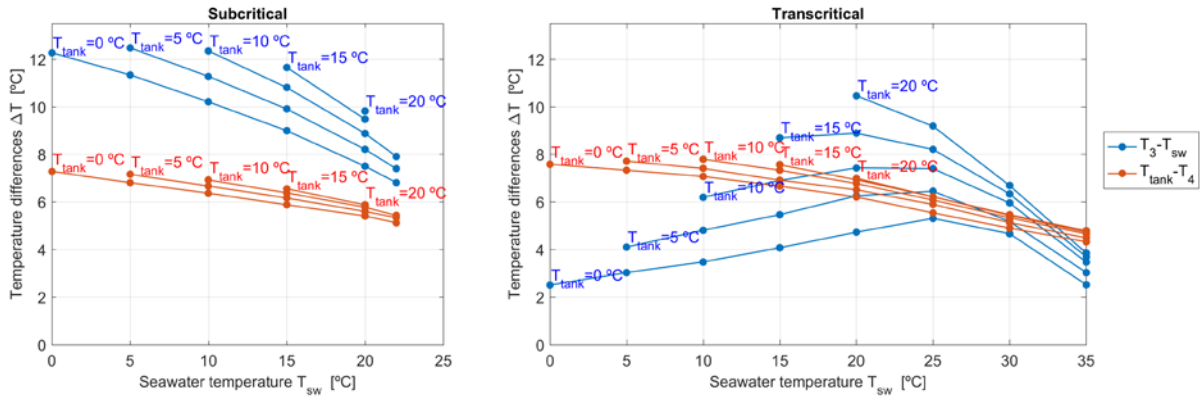


Figure 6. Temperature differences in the gas cooler (blue) and evaporator (red).

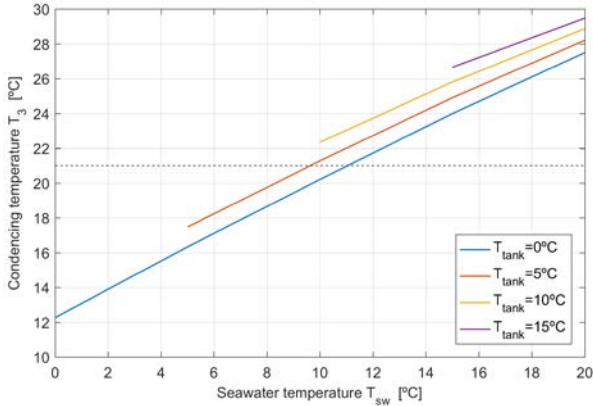


Figure 7. Condensing temperature  $T_3$  in the subcritical process.

Table 3 shows that the pressure drop over the evaporator is low compared to the system operating conditions, as a consequence the evaporation temperature at suction pressure is similar to the inlet evaporator temperature ( $T_E \approx T_4$ ), which is also illustrated in Figure 4. Figure 6 shows that the difference ( $T_{\text{tank}} - T_4$ ) is between 5° C and 7° C for all cases where  $T_{\text{tank}} = 20^\circ \text{C}$ . That is, a maximum  $T_4$  of 15° C, which is close to the compressor limit ( $T_E \leq 15^\circ \text{C}$ ). Hence,  $T_{\text{tank}} \leq 20^\circ \text{C}$  will be considered as a limit for the RSW system. Modeling performance outside the compressor range is based on extrapolation because the polynomial fitted compressor data in Eqs. (4) – (7) are not valid outside the compressor limit curve. Figure 8 shows a COP optimized 2D presentation of the data in Figure 5 using cubic interpolation and linear extrapolation at  $T_{\text{tank}} > 20^\circ \text{C}$  from the “ $T_{\text{tank}} \leq 20^\circ \text{C}$ ” data.

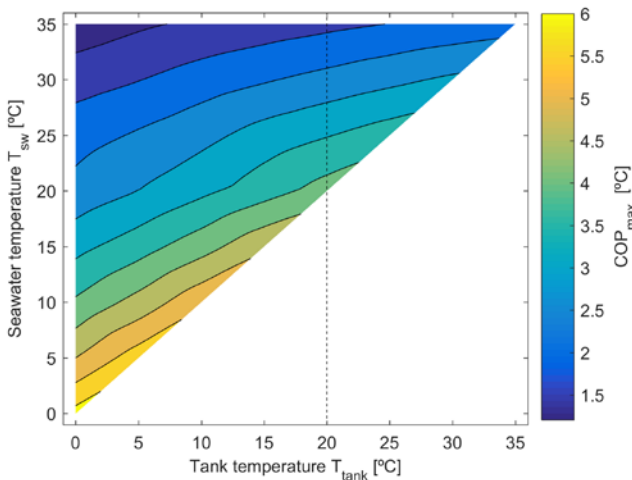


Figure 8. Maximum COP at different tank temperatures. Compressors operate outside the limit curve if  $T_{\text{tank}} > 20^\circ \text{C}$ .

### 3.2 Transient Chilling and Performance

Figure 9 illustrates how the tank temperature and COP vary in time for the “Case A” filling scenario at different seawater temperatures. Figure 10 shows the results for “Case B”. Note that the temperature change is nonlinear as e.g. illustrated for “Case A” with  $T_{sw} = 30^\circ\text{C}$ , where it takes approximately one hour to cool the RSW tank from 30 to  $20^\circ\text{C}$ , while it takes about 1.5 hours from 10 to  $0^\circ\text{C}$ . These figures also show average COP and  $P_E$  for each process. Processes operating outside the compressors range are shown as dotted lines in Figure 9, and were computed from the extrapolated values shown in Figure 8. A simple refrigeration process without precooling (“Case A”) was chosen to emphasize the importance of implementing equipment to regulate the evaporator pressure in warm climates. Working outside compressor design range is avoided (for longer time periods) in “Case B”, by regulating the RSW tank’s water supply in the precooling stage.

The overall performance, described by the average  $\text{COP}_{av}$  and the maximum RSW tank volume ( $V_{\text{tank}}^{\text{max}}$ ) which can be cooled according to food industry regulations, are summarized in Figure 11.

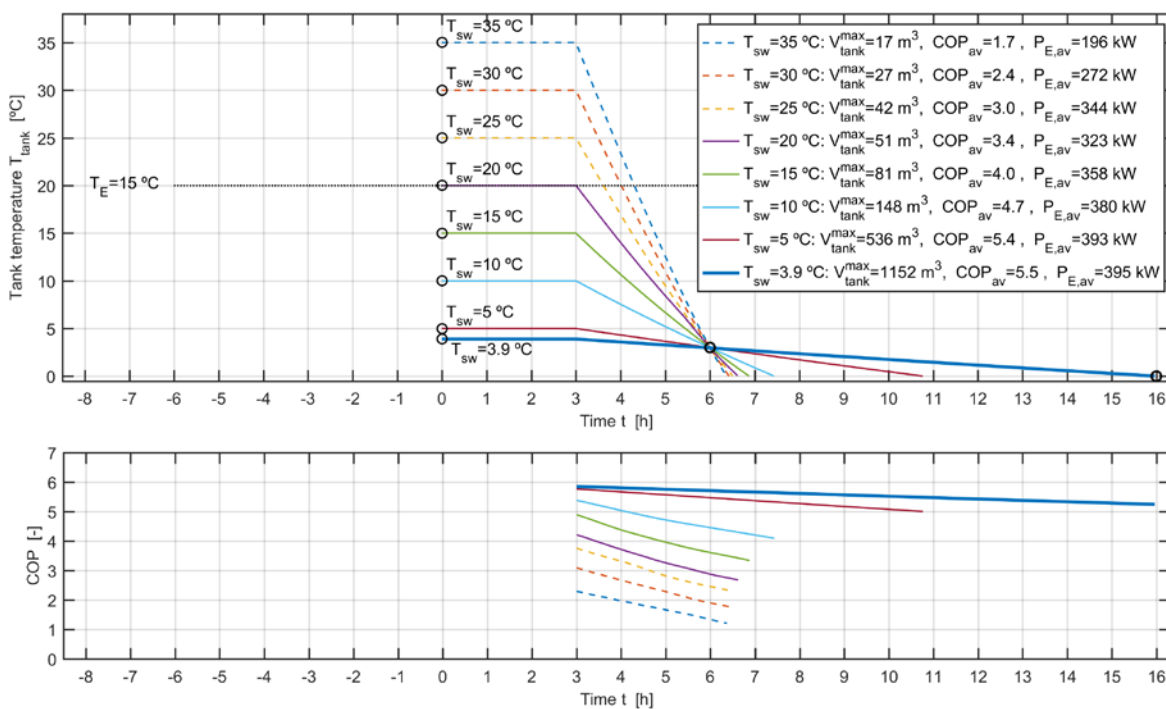


Figure 9. Tank temperature (top) and COP (bottom) as functions of time for “Case A”. Dashed lines are not recommended for the compressor, due to high evaporating temperature.

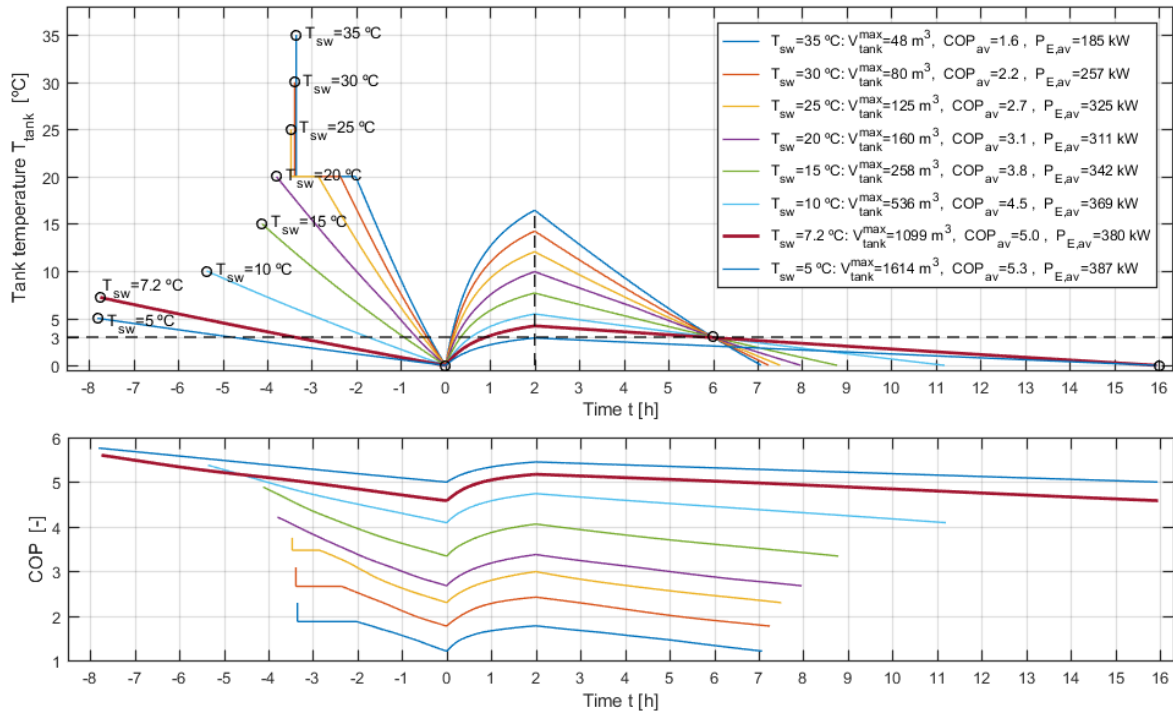


Figure 10. Temperature (top) and COP (bottom) as functions of time. “Case B”: RSW cooling process using maximum RSW tank size ( $V_{tank}^{max}$ ) possible when precooling of 1/3 water. Seawater/fish is added during two hours, starting at time  $t=0$ .

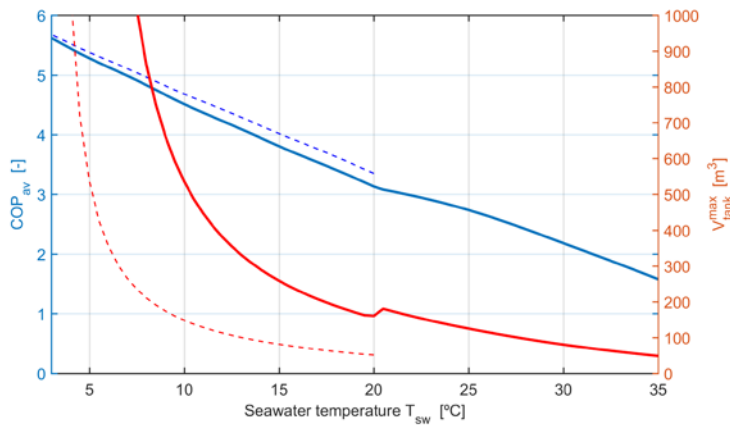


Figure 11. Average COP (blue) and maximum RSW tank size (red) for the two different cooling processes; “Case A” (dotted lines) and “Case B” (solid lines). Only processes within the operating range of the compressors are shown.

### 3.3 Performance at Different Geographical Locations

The maximum RSW tank volume is limited by food industry regulations. Figure 12 shows how the maximum volume varies with geographic location for “Case A” for the “worst case scenario” based on maximum sea surface temperatures ( $SST_{max}$ ). The energy efficiency is described by the yearly average ( $COP_{av}$ ), calculated from the average sea surface temperatures ( $SST_{av}$ ). Figure 13 shows how this parameter varies with geographic location for “Case B” with precooling of water.



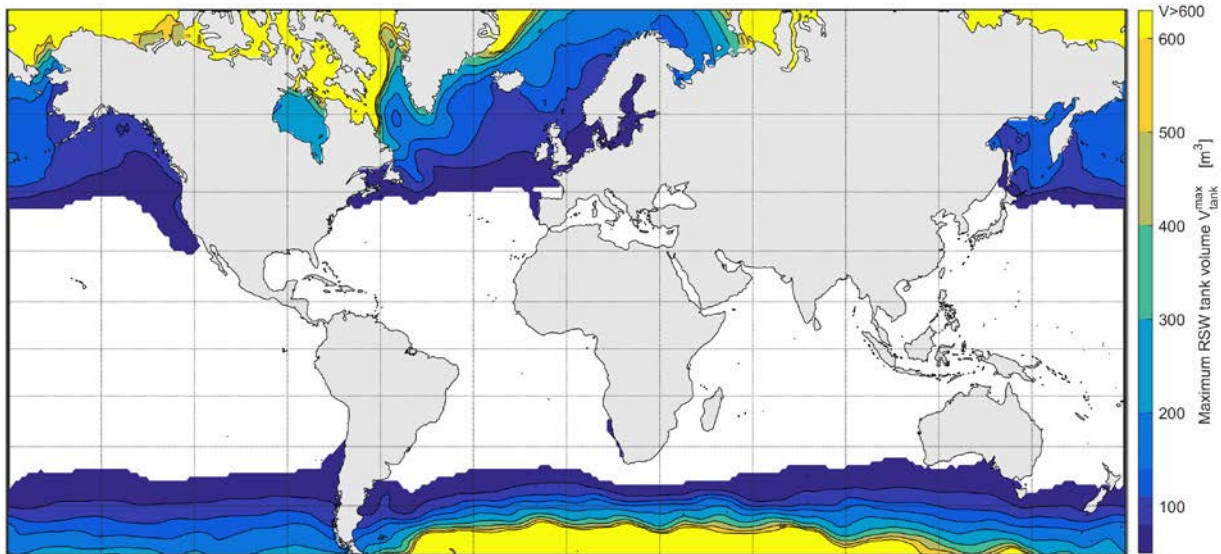


Figure 12. Maximum RSW tank volume for “Case A” filing during the warmest period of the year. The  $SST_{max}$  is above  $20^{\circ}C$  in the white regions, i.e. above the  $CO_2$  compressor’s operating range.

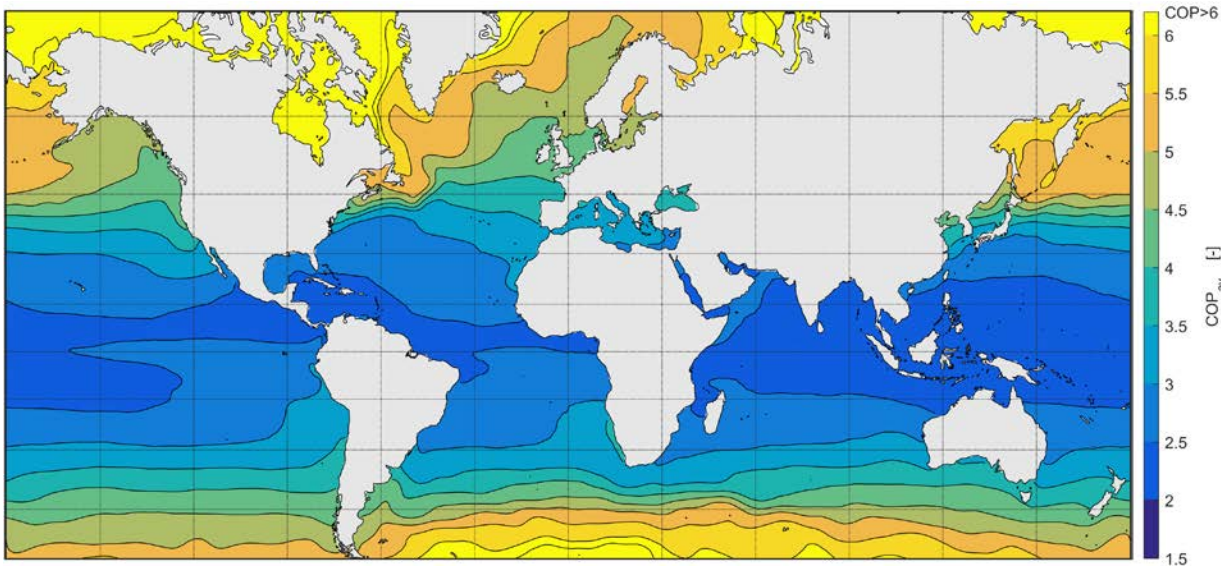


Figure 13. Average COP for “Case B” filling with precooling. Calculated using average sea surface temperatures ( $SST_{av}$ ).

## 4 Discussion

The modelling work conducted here is based on property predictions made using the Peng Robinson (PR) equation of state. The application of PR in HYSYS was chosen to facilitate the selected modelling approach for heat exchangers and the compressor. The accuracy with which PR predicts thermodynamic properties for  $CO_2$  is lower than some alternatives, particularly in the region  $300 < T < 308 K$  and  $70 \text{ bar} < p < 78 \text{ bar}$  close to the critical point (Wilhelmsen et al., 2012). However, since RSW operating cases close to the critical point have relatively poor COP, the optimization routine used in modelling process finds no optimum cases close to the critical point. In this study, for example, all transcritical processes have  $p_3 > 82 \text{ bar}$ . As long as the region directly around the critical point is avoided, the average error in property predictions should be less than 5% (Wilhelmsen et al., 2012). This level of absolute accuracy is

considered acceptable in the present study where relative performance of a fixed refrigeration system design is the focus.

The RSW system performance depends on the seawater temperature, the tank filling scenario, the RSW design and the equipment used, e.g. heat exchanger sizes. There are many possible RSW designs. This article only investigates one particular design with relatively few components. Real RSW systems typically have more complex designs to improve energy efficiency and reduce capital cost. For example, Figure 4 shows that more than 1/5 of the evaporator area is used for the 4 K superheating to protect the compressor. That is, the evaporator's heat transferring area could be reduced, or used more efficiently, if a suction gas heat exchanger is included (Boewe et al., 2001). Ejectors can also be included to reduce throttling loss (Lucas and Koehler, 2012; Haida et al., 2016). A CO<sub>2</sub> cycle with few components was modeled with the aim of creating a basis that was simple and transparent and provided a consistent basis to illustrate general trends in RSW system performance.

The CO<sub>2</sub> based RSW systems from Kuldeteknisk AS are called SeaCool, and have cooling capacities from 79 to 430 kW (Kuldeteknisk AS, 2017). Two temperature cases are specified for each model, where the largest model has 346 kW cooling capacity with 104.8 kW compressor consumption (COP=3.30) when  $T_{\text{tank}} = 0^{\circ}\text{C}$  and  $T_{\text{sw}} = 15^{\circ}\text{C}$ , and 430 kW cooling capacity with 157.8 kW compressor consumption (COP=2.72) when  $T_{\text{tank}} = 0^{\circ}\text{C}$  and  $T_{\text{sw}} = 20^{\circ}\text{C}$  (Kuldeteknisk AS, 2017). This supports the modeling approach, where the corresponding COP values are 3.34 and 2.67, respectively (see Figure 5). That is, the difference is less than 3%, which is probably less than the accuracy of the Peng Robinson based model for CO<sub>2</sub> (Wilhelmsen et al., 2012). However, the small differences imply that the simple RSW system modeled here, to some extent, compensates efficiency loss in inefficient processes with improved (larger or cleaner) heat exchangers.

The RSW process can be viewed in two stages: firstly chilling fish and seawater to 0° C, and secondly keeping the RSW tank temperature at 0° C. Only the first stage is modeled here, and it is assumed that the compressors are working at full load. Reduced compressor loads affect the performance, and modeling this is outside the scope of this work. The energy consumption in the second stage is not considered because it is relatively small. Cooling capacity needed is typically only a fraction after reaching 0° C, e.g. the heat transfer loss for the RSW tank in Båragutt MS is estimated to 25 kW, which is 6 % of the full load chilling duty (Gilberg, 2011). The modelling basis includes the assumption that RSW circulation is constant, which results in longer recirculation time for larger tanks. The basis also assumes that there is no temperature gradient across the RSW tanks, but with longer recirculation time this is less easy to guarantee. Although, these two assumptions are potentially incompatible, the modelling work is also based on a fixed RSW unit size, which means that large RSW tank cases only occur where the start temperature is low and significant temperature gradients could not exist.

Precooling – efficiency versus capacity. Two different RSW cooldown processes to 0° C (“Case A” and “Case B”) have been modelled. These processes are shown in Figure 9 and Figure 10 for different seawater temperatures. “Case A” starts the refrigeration cycle when the tank is full (after three hours), i.e., warm and cold water are not mixed during the process, which is the most efficient way of cooling the RSW tank content. In “Case B” 1/3 of the RSW tank is pre-cooled to 0° C before fish are added. This process was chosen as scenario for the upper volume limit for an RSW tank that the refrigeration unit can operate using precooling, given that at least 2/3 of the RSW tank is dedicated to fish. Although a limited set of scenarios are studied here, the comparisons made provide important insight into the performance of RSW systems.

Energy efficiency is higher in cold locations. Figure 13 shows that a CO<sub>2</sub> based RSW unit can achieve large COP in polar regions and that there is a significant reduction in energy efficiency if operated in warm



seawater. The COP is typically more than 4.0 in Northern Europe, above 5.0 in the Barents Sea and only 3.0 to 3.5 in the Mediterranean Sea. Precooling reduces COP, but only slightly, as illustrated in Figure 11. Between “Case A” and “Case B”, there is only a 6.8% reduction at 20° C SST and 1.3% reduction at 3° C SST. COP during the cooldown process are shown in Figure 9 and Figure 10 for different seawater temperatures.

Maximum RSW tank size depends on SST and increases with precooling, and is related to the EU Council Directive (92/48/EEC), which states that the fish must reach 3° C at most six hours after loading and 0° C at most sixteen hours after loading. The first condition is typically the one limiting the maximum tank size the refrigeration unit can cool down, as illustrated in Figure 9 and Figure 10. However, in cold waters the last condition limits the maximum size of the tank, which occurs if the SST below 3.9° C for “Case A” and below 7.2° C for “Case B”. Figure 11 shows that the maximum water that can be cooled in one tank is increased with precooling, i.e. “Case B” can cool 3.0 times more water than “Case A” at 20° C SST and 3.6 times more at 10° C SST. Figure 9 – Figure 11 show that fishing boats can operate with RSW tanks that are about 3 times larger if SST is 10° C instead of 20° C. Figure 12 shows the maximum volume that can be cooled down in one tank at different locations, and the regions where the RSW unit can not start to cool down a full RSW tank due to compressor limitations ( $T_E \leq 15^\circ \text{C}$ ). However, the total amount of water that can be cooled down is increased if more than one tank is serviced by the same RSW unit.

Ships equipped with CO<sub>2</sub> based RSW must be able to operate transcritical if they are expected to operate in warm waters. For the RSW system studied here, a subcritical process is only possible if seawater is below 22° C, and Figure 5 shows that transcritical processes are more efficient above 20° C.

A means of regulating the evaporator pressure is unnecessary in cold climates, but needed in warm regions as illustrated in Figure 11 and Figure 12. CO<sub>2</sub> compressors are currently designed for relatively low evaporating temperatures ( $T_E$ ) where CO<sub>2</sub> based refrigeration systems can compete on performance. If the RSW pump is automatically regulated to reduce the water flow through the evaporator in warm waters, the RSW unit could cool a full tank at any seawater temperature, but at a reduced COP and cooling capacity.

The results of this study show that traditional modelling assumptions may underplay the performance of CO<sub>2</sub> based systems. Comparisons based simply on condensing and evaporating temperatures are likely to underestimate the performance of CO<sub>2</sub> based systems, which operate at a higher density and pressures relative to HCFC-22 and other alternative refrigerants, resulting in good heat transferring coefficients. Figure 4 also shows that the pinch point for a transcritical process lies at the cold end of the exchanger instead of in the middle of the exchanger, which is the case for a subcritical process. This makes lower temperature approached possible and is an important benefit of the transcritical process. For example, Figure 6 shows that for  $T_{\text{tank}} = 0^\circ \text{C}$ , the gas cooler temperature differences ( $T_3 - T_{\text{sw}}$ ) are between 2 K to 5 K (transcritical), which is much smaller than the 13.5 K used by Pigani et al., 2016. The study by Pigani et al. only considered transcritical CO<sub>2</sub> based systems, while all the other refrigerants they studied were running subcritical. Their study does therefore not account for the benefits of subcritical CO<sub>2</sub> based operations at lower SST.

Not all literature agrees that CO<sub>2</sub> is a good refrigerant. Pigani et al. concluded that none of the low GWP refrigerants offered maintained or improved efficiency (Pigani et al., 2016), but this study only includes cases with high seawater temperatures with condensing temperatures above 31.5° C. Hansen has claimed that CO<sub>2</sub> is more efficient than HCFC-22 when the condensing temperature is less than 21° C (Hansen, 2000). Figure 7 shows that for the modeled RSW unit this occurs when the seawater is below 10° to 11° C. Figure 11 shows that this average SST corresponds to  $\text{COP}_{\text{av}} \approx 4.5$  and corresponds geographically to the sea temperatures found between Denmark and Norway as illustrated in Figure 13.

However, this study highlights the flaw of comparing the performance of different refrigerants without taking into account heat exchanger performance. More work should be done to investigate this more accurately.

## 5 Conclusion

Refrigeration and cooldown processes for a CO<sub>2</sub> based RSW unit with a fixed design, size and equipment have been modeled using real compressor data and a sophisticated approach to heat exchanger modelling. The modelled performance matches available performance data for a real system Kuldeteknisk AS, 2017 and shows that CO<sub>2</sub> based RSW units perform well in cold climates. Figure 13 shows that while the average COP is above 5.0 in the Barents Sea, it is only 3.0 to 3.5 in the Mediterranean Sea. The performance is highly sea temperature dependent since CO<sub>2</sub> based systems have to operate close or above the critical pressure in warm climates. The evaporator pressure must also be regulated to avoid operating outside the compressor specifications in warm climates like Southern Europe.

Precooling of water in the RSW tank introduces mixing of water/fish with different temperature, which will result in reduced COP. However, this study shows that the difference in average COP, with or without precooling, is less than 7 % for cooling processes from 20° to 0° C, and that average COP are almost identical in cold regions. However, the RSW tank can be 3.6 to 1.8 times larger if precooling 1/3 of the RSW tank water before adding the fish load if following EU Directive requirements. The maximum load in one RSW tank at different seawater temperatures is illustrated in Figure 11, and shows that fishing boats can operate a 3 – 3.5 times larger RSW tank if the seawater is 10° C instead of 20° C.

Comparative studies with CO<sub>2</sub> and other refrigerants often operate with simplified heat exchanger models assuming a constant temperature difference, i.e. the same value for all refrigerants, for both transcritical and subcritical processes. The temperature differences ( $T_3 - T_{sw}$ ) modeled for the gas cooler was found to be much smaller than e.g. used by Pigani et al., 2016, particularly in the transcritical processes. The smaller temperature approaches found for the gas cooler suggests that much literature is likely to underestimate CO<sub>2</sub> as a refrigerant choice.

## REFERENCES

- Boewe, D. E., Bullard, C. W., Yin, J. M., Hrnjak, P. S., 2001. Contribution of internal heat exchanger to transcritical R744 cycle performance. *Int J Hvac&R Research* 7(2): 155-168.
- EU Council Directive (92/48/EEC), 1992. Official Journal of the European Communities.
- Gilberg, A. F., 2011. Development of a CO<sub>2</sub> RSW system onboard a fishing vessel (Master of Science in Engineering and ICT). Norwegian University of Science and Technology, Trondheim.
- Haida, M., Banasiak, K., Smolka, J., Hafner, A., Eikevik, T. M., 2016. Experimental analysis of the R744 vapour compression rack equipped with the multi-ejector expansion work recovery module. *International Journal of Refrigeration* 64: 93-107.
- Hansen, T. M., 2000. Alternatives to HCFC as refrigerant in shipping vessels. Ekspressen Tryk & Kopicenter, Copenhagen.

Japan Meteorological Agency. Monthly average SST data are posted on the Tokyo climate center website at: <[http://ds.data.jma.go.jp/tcc/tcc/products/el\\_nino/cobesst\\_doc.html](http://ds.data.jma.go.jp/tcc/tcc/products/el_nino/cobesst_doc.html)> (accessed 03.03.17).

Japan Meteorological Agency, 2006. Characteristics of global sea surface temperature analysis data (COBE-SST) for climate use. Monthly report on climate system separated 12.

Kim, M.-H., Pettersen, P., Bullard, C. W., 2004. Fundamental process and system design issues in CO<sub>2</sub> vapor compression systems. *Progress in Energy and Combustion Science* 30: 119-174.

Kolbe, E., 1990. Refrigeration energy prediction for flooded tanks on fishing vessels. *Applied Engineering in Agriculture* 6(5).

Kuldeteknisk AS. Technical data (Version 2.1 and 2.0) <[www.kuldeteknisk.no](http://www.kuldeteknisk.no)> (accessed 04.03.17).

Lindeburg, M. R., 2013. *Chemical Engineering Reference Manual*. Professional Publications, Inc., California.

Lucas, C., Koehler, J., 2012. Experimental investigation of the COP improvement of a refrigeration cycle by use of an ejector. *International Journal of Refrigeration* 35: 1595-1603.

Pedersen, P. H., 2014. HCFC phase out in the Nordic countries. *Nordic Working Papers*, Copenhagen.

Pigani, L., Boscolo, M., Pagan, N., 2016. Marine refrigeration plants for passenger ships: Low-GWP refrigerants and strategies to reduce environmental impact. *International Journal of Refrigeration* 64: 80-92.

Ruiz, V., 2012. Analysis of existing refrigeration plants onboard fishing vessels and improvement possibilities. *Second International Symposium on Fishing Vessel Energy Efficiency, E-Fishing*.

Sharqawy, M. H., Lienhard, J. H., Zubair, S. M., 2010. Thermophysical properties of seawater: A review of existing correlations and data. *Desalination and Water Treatment* 16: 354-380.

Skiple, T., 2008. Utfasing av R22 i fiskefartøy. SINTEF Energiprosesser, Trondheim.

Thorsteinsson, J. A., Jensson, P., Condra, T. J., Valdimarsson, P. 2003. Transient simulation of refrigerated and chilled seawater system. *Proceedings of the 44th Conference on Simulation and Modelling*, Vesteraas.

Tveit, G. M., Digre, H., Aursand, I., Solvang-Garten, T., Eilertsen, A., Schei, M., 2015. Overpumping av makrell – Effekt på fangstkvalitet. SINTEF Fiskeri og havbruk AS, Råstoff og prosess.

United Nations Environment Programme (UNEP), 2006. *Montreal protocol on substances that deplete the ozone layer*. Nairobi, Kenya.

Wang, S. G., Wang, R. Z., 2005. Recent developments of refrigeration technology in fishing vessels. *Renewable Energy* 30: 589-600.

Widell, K. N., Eikevik, T., 2010. Reducing power consumption in multi-compressor refrigeration systems. *International Journal of Refrigeration* 33: 88-94.

Wilhelmsen, Ø., Skaugen, G., Jørstad, O., Li, H., 2012. Evaluation of SPUNG and other equations of state for use in carbon capture and storage modelling. *Energy Procedia* 23: 236-245.

Wolf, S. R. L., 2015. DORIN Software, version 15.07.